Lubricating bacteria model for branching growth of bacterial colonies

Yonathan Kozlovsky, Inon Cohen, Ido Golding, and Eshel Ben-Jacob
School of Physics and Astronomy, Raymond and Beverly Sackler Faculty of Exact Sciences, Tel Aviv University, Tel Aviv 69 978, Israel
(Received 9 September 1998; revised manuscript received 17 February 1999)

Various bacterial strains (e.g., strains belonging to the genera *Bacillus, Paenibacillus, Serratia,* and *Salmonella*) exhibit colonial branching patterns during growth on poor semisolid substrates. These patterns reflect the bacterial cooperative self-organization. A central part of the cooperation is the collective formation of a lubricant on top of the agar which enables the bacteria to swim. Hence it provides the colony means to advance towards the food. One method of modeling the colonial development is via coupled reaction-diffusion equations which describe the time evolution of the bacterial density and the concentrations of the relevant chemical fields. This idea has been pursued by a number of groups. Here we present an additional model which specifically includes an evolution equation for the lubricant excreted by the bacteria. We show that when the diffusion of the fluid is governed by a nonlinear diffusion coefficient, branching patterns evolve. We study the effect of the rates of emission and decomposition of the lubricant fluid on the observed patterns. The results are compared with experimental observations. We also include fields of chemotactic agents and food chemotaxis and conclude that these features are needed in order to explain the observations. [S1063-651X(99)03406-6]

PACS number(s): 87.10.+e, 47.20.Hw

I. INTRODUCTION

It is now understood that the study of cooperative self-organization of bacterial colonies is an exciting new multidisciplinary field of research, necessitating the merger of biological information with the physics of nonequilibrium processes and the mathematics of nonlinear dynamics. At this stage, several experimental systems have been identified, and preliminary modeling efforts are making significant progress in providing a framework for the understanding of experimental observations [1–13].

In nature bacterial colonies must often cope with hostile environmental conditions. To do so, bacteria have developed sophisticated cooperative behavior and intricate communication capabilities [14–18]. These include direct cell-cell physical interactions via extra-membrane polymers [19,20], collective production of extracellular ''wetting'' fluid for movement on hard surfaces [1,21], long-range chemical signaling, such as quorum sensing [22–24] and chemotactic signaling [25–27], collective activation and deactivation of genes [28,29,2], and even exchange of genetic material [30–32]. Utilizing these capabilities, bacterial colonies develop complex spatio-temporal patterns in response to adverse growth conditions.

For researchers in the pattern formation field, the above communication mechanisms open a new class of tantalizing complex models exhibiting a much richer spectrum of patterns than the models of nonliving systems.

Fujikawa and Matsushita [4,33,34] reported for the first time (by which we mean the first time that branching growth was studied as such; observations of branching colonies occurred long ago [35,36]) that bacterial colonies could grow elaborate branching patterns of the type known from the study of fractal formation in the process of diffusion-limited-aggregation (DLA) [37–39]. This work was done with *Bacillus subtilis*, but was subsequently extended to other bacterial species such as *Serratia marcescens* and *Salmonella anatum* [40].

Motivated by these observations, Ben-Jacob *et al.* conducted new experiments with a new species of bacteria that has been isolated from cultures of *Bacillus subtilis* [6,41,8]. The new species was designated *Paenibacillus dendritiformis* var. *dendron* [42]. This species is motile on the hard surface and its colonies exhibit branching patterns (Fig. 1). The new mode of tip-splitting growth was found to be inheritable and transferable by a single cell, hence it is referred to as a distinctive morphotype [43], and, to indicate the tip-splitting character of the growth, it was denoted $\mathcal{T}$ morphotype. In the next section we describe in some detail the observations of Ben-Jacob *et al.* Additional studies of branching colonial growth are reported by Matsuyama *et al.* [1,44] and Mendelson and Salhi [2].

How should one approach the modeling of the complex bacterial patterning? With present computational power it is natural to use computer models as a main tool in the study of complex systems. However, one must be careful not to be trapped in the ''reminiscence syndrome,'' described by Cowan [45], as the tendency to devise a set of rules which will mimic some aspect of the observed phenomena and then, to quote Cowan, ''They say: 'Look, isn't this reminiscent of a biological or physical phenomenon!' They jump in right away as if it's a decent model for the phenomenon, and usually of course it's just got some accidental features that make it look like something.'' Yet the reminiscence modeling approach has some indirect value. True, doing so does not reveal (directly) the biological functions and behavior. However, it does reflect understanding of geometrical and temporal features of the patterns, which indirectly might help in revealing the underlying biological principles. Another extreme is the ''realistic modeling'' approach, where one constructs an algorithm that includes in detail all the known biological facts about the system. Such an approach sets a trajectory of ever including more and more details (versus generalized features). The model keeps evolving to include so many details that it loses any predictive power.

Here we try to promote another approach—the ''generic modeling'' one [46,8,47,12]. We seek to elicit, from the experimental observations and the biological knowledge, the

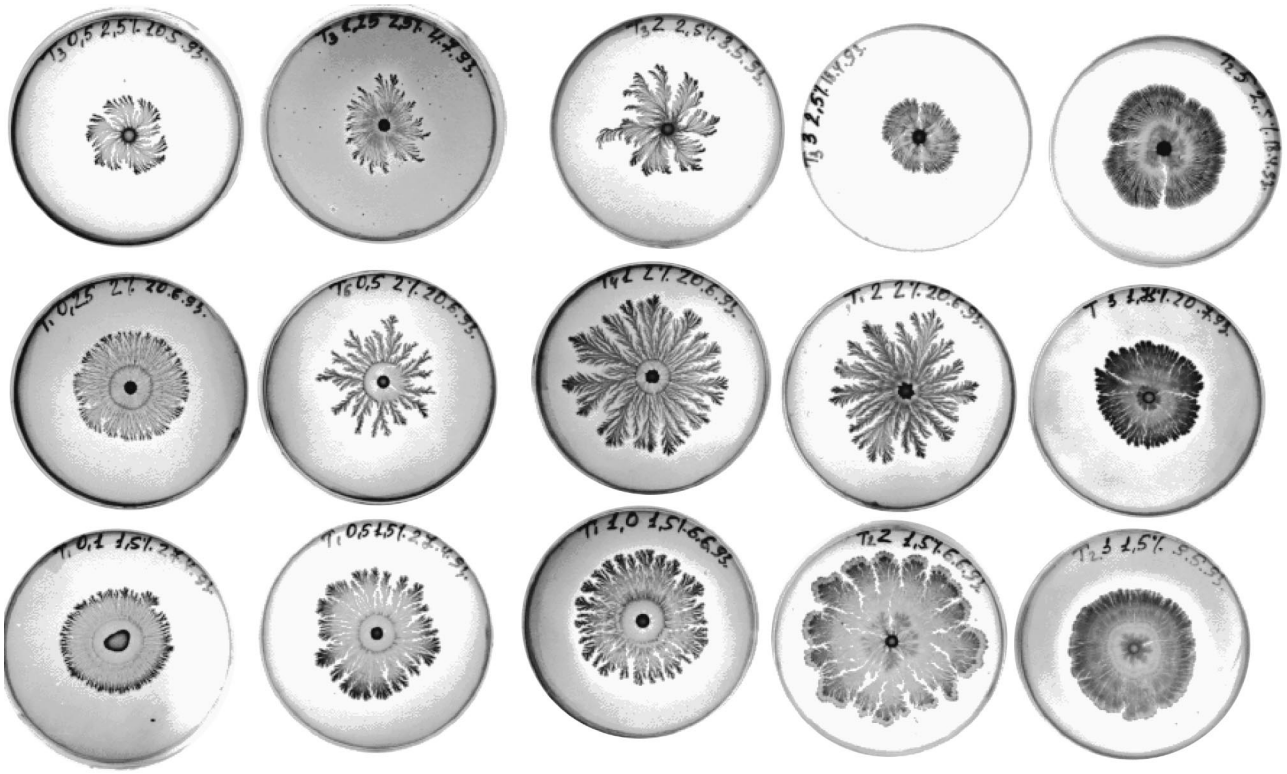

(a)

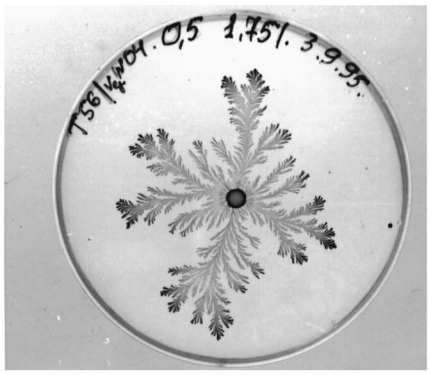

(b)

FIG. 1. (a) A diagram of colonial branching patterns of the bacteria *Paenibacillus dendritiformis* var. *dendron*. The dot at the center of each colony is the initial inoculum. The horizontal axis of the diagram is initial nutrient concentration. From left to right (in units of g/l) it is 0.1, 0.5, 1.0, 2.0, and 3.0 . The vertical axis is agar concentration. From bottom to top (in units of 10 g/l) it is 1.5, 2, and 2.5 . As the level of initial nutrient concentration is decreased, the patterns become less organized with fewer branches. However, at the lowest concentration, of 0.1 g/l, the pattern is ordered with circular envelope. (b) An isolated example of branching pattern at 0.5 g/l pepton and 1.75% agar concentration.

generic features and basic principles needed to explain the biological behavior and to include these features in the model. We will demonstrate that such modeling, with close comparison to experimental observations, can be used as a research tool to reveal new understanding of the biological systems.

Generic modeling is not about using ''sophisticated'' mathematical description to address preexisting understanding of complex biological behavior. Rather, it means a cooperative approach, using existing biological knowledge together with mathematical tools and a synergetic point of view for complex systems to reach a new understanding (which is reflected in the constructed model) of the observed complex phenomena.

The generic models can yet be grouped into two main categories. (i) Discrete models such as the communicating walkers models of Ben-Jacob *et al.* [8,48,11] and the bions model of Kessler and Levine [46,49]. In this approach, the micro-organisms (bacteria in the first model and amoebae in second) are represented by discrete, moving entities (walkers and bions, respectively) which can consume nutrients, reproduce, perform random or biased movement, and produce or respond to chemicals. The time evolution of the chemicals is described by reaction-diffusion equations. (ii) Continuous or reaction-diffusion models [50,51]. In these models the micro-organisms are represented via their two-dimenstional (2D) density, and a reaction-diffusion equation of this density describes their time evolution. This equation is coupled

to the other reaction-diffusion equations for the chemical fields. In the context of branching growth, this idea has been pursued recently by Matsushita *et al.* [52], Kawasaki *et al.* [53], and Kitsunezaki [54]. A summary and critique of this approach is provided by Rafols [55].

One of the important features of the bacterial colonies is the lubricant layer in which the bacteria swim. A model for the colony should include this feature, directly or indirectly [17,56]. Here we present a model which specifically includes the lubricant excreted by the bacteria. The model follows the second approach of generic modeling. We represent the various entities: the bacteria, the chemicals, and the lubricant by continuous fields.

II. EXPERIMENTAL AND BIOLOGICAL BACKGROUND

In Fig. 1(a) we show branching patterns of bacterial colonies. Each of these colonies is made up of about 10^{10} bacteria of the type *Paenibacillus dendritiformis* var. *dendron* (see [6,41] for first reference in the literature and [42] for identification). Each colony is grown in a standard petri dish (8 cm in diameter) on a thin layer of agar (semi-solid jelly). Figure 2(a) shows that the branches of the colonies have a well defined boundary, and the bacteria are confined by this boundary. Figures 2(b) and 2(c) highlight the constituents of the branches. Figure 2(b) shows that each branch is a layer of fluid on the surface of the agar. Figure 2(c) shows the bacteria, all of which are confined within this fluid. The bacteria cannot move on the dry surface and cooperatively they produce a layer of lubrication fluid in which they swim.

Bacterial swimming is a random-walk-like movement, in which the bacteria propel themselves in nearly straight runs separated by brief tumbling. Swimming can be done only in a fluid with low viscosity. To produce such fluid the bacteria secrete lubricant (wetting agents). Other bacterial species produce known extracellular lubricants (such as surfactants, see [1,57–59] and references therein, or the extracellular slime produced by *Proteus mirabilis* [60]). These are various materials (various cyclic lipopeptides were identified) which draw water from the agar. The composition and properties of the lubricant of *P. dendritiformis* are not known, but we will assume that a higher concentration of lubricant is needed to extract water from a dryer agar, and that the lubricant is slowly absorbed into the agar (or decomposes).

In order to move, reproduce, and perform other metabolic activities, the bacteria consume nutrients from the media, nutrients which are given in limited supply. The growth of a colony is limited by the diffusion of nutrients towards the colony—the bacterial reproduction rate that determines the growth rate of the colony is limited by the level of nutrients available for the cells. If the nutrient is deficient for a long enough period of time, the bacteria may enter a prespore state, i.e., begin the process of sporulation. They stop normal activity—like movement—and use all their internal reserves to metamorphose from an active motile cell to a spore—sedentary durable ''seed.'' The sporulating bacteria emit a wide range of materials, some of which are unique to the sporulating bacteria. These emitted chemicals might be used by other bacteria as a signal carrying information about the conditions at the location of the prespores.

The patterns in Fig. 1(a) are arranged in a diagram according to two control parameters: the initial concentration of nutrients (horizontal axis, increasing from left to right), and the concentration of the agar, or the dryness of the media (vertical axis, increasing from bottom to top). The chirality of the colonies at the top row is due to interaction between repulsive chemotaxis (see Sec. V) and the process of tum-

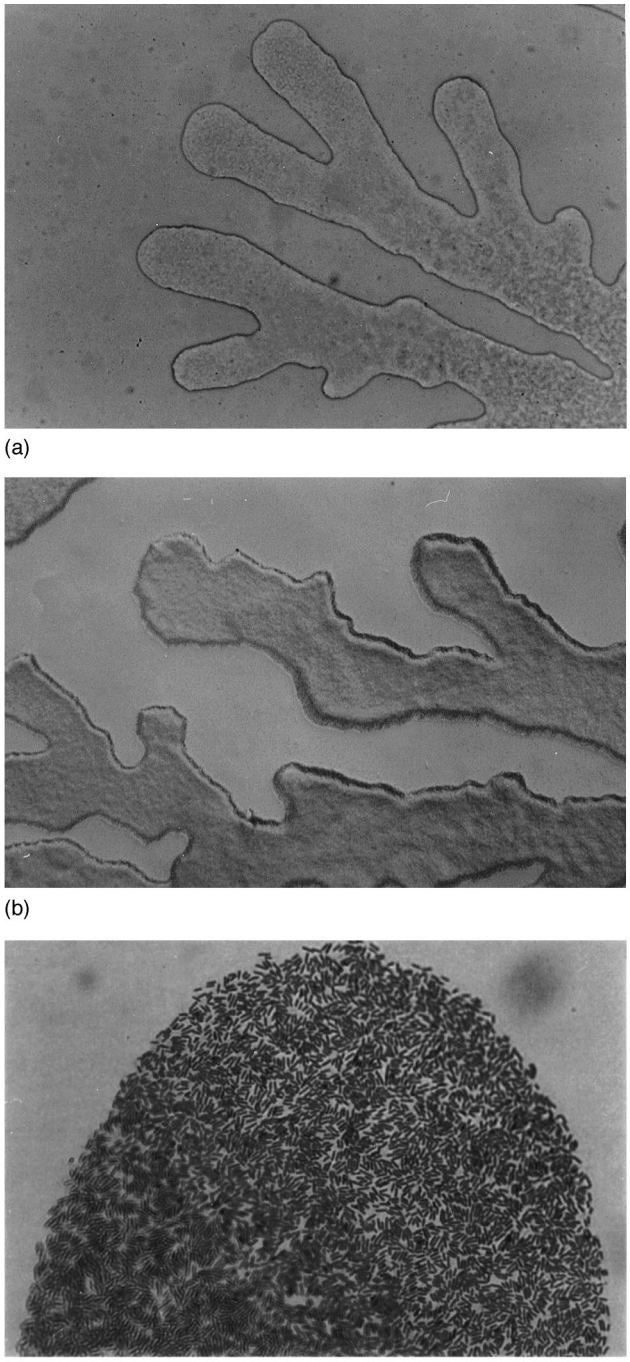

FIG. 2. Closer look on branches of a colony. (a) $\times 20$ magnification shows the sharp boundaries of the branches. The width of the boundary is in the order of microns. (b) Numarsky (polarized light) microscopy shows the height of the branches and their envelope. What is actually seen is the layer of lubrication fluid, not the bacteria. (c) $\times 50$ magnification shows the bacteria inside a branch. Each bar is a single bacterium. There are no bacteria outside the branch.

bling (see Refs. [48,16] for details). It will be ignored in this paper. For a high level of initial nutrient concentration (right column), the patterns are compact, with wide branches. For intermediate levels of nutrients, the lower the initial concentration is, the more ramified and less ordered the patterns are. The patterns become fractal-like, with fractal dimension decreasing for lower levels of nutrients. For the same nutrient level, higher agar concentration makes the branches thinner. The above phenomena could be expected from our knowledge on patterning in nonliving systems [61–64,16]. Unlike what could have been expected, at the lowest concentration of nutrient (leftmost column), the patterns are more ordered with a well defined circular envelope. Those patterns are characterized as fine radial branches. This phenomenon demonstrates the complexity of the biological system, and its explanation needs an additional biological feature—chemotaxis signaling (see Sec. V). Figure 3 demonstrates that in spite of this complexity and the inherent noise in the system, the experiments are controlled enough for the patterns to be reproducible.

FIG. 3. Demonstration of the reproducibility of the colonial patterns. Four colonies in the same plate (from four inocula).

III. CONSTRUCTION OF THE MODEL

The model includes four coupled fields projected on 2D. One field describes the density of motile bacteria $b(\vec{x},t)$, the second describes the height of the lubricant layer in which the bacteria swim $l(\vec{x},t)$, the third field describes the concentration of nutrients $n(\vec{x},t)$, and the fourth field is the density of stationary bacteria $s(\vec{x},t)$, bacteria that enter the prespore state.

We first describe the dynamics of the bacteria and of the nutrient. The two reaction-diffusion equations governing those fields have the following form:

$$\frac{\partial b}{\partial t} = \text{movement} + \text{reproduction} - \text{sporulation},$$
$$\frac{\partial n}{\partial t} = \text{diffusion} - \text{consumption}. \tag{1}$$

The sporulation term refers to the transition of motile bacteria into the stationary state, i.e., the prespore state. The nutrient diffusion is a simple diffusion process with a constant diffusion coefficient. The rate of nutrient consumption is proportional to the rate of bacterial reproduction. For the reproduction term in Eq. (1) we take

$$\text{reproduction} = knb, \tag{2}$$

where k is a constant rate. This is the usual form included in reaction-diffusion models, but see Sec. VI for a more detailed discussion. The exact form of the sporulation term is not known. For simplicity we take the form

$$\text{sporulation} = \mu b, \tag{3}$$

where the rate μ is constant.

We now turn to the bacterial movement. In a uniform layer of liquid, bacterial swimming is a random walk with variable step length and can be approximated by diffusion. The layer of lubricant is not uniform, and its height affects the bacterial movement. An increase in the amount of lubricant decreases the friction between the bacteria and the agar surface. The term ''friction'' is used here in a very loose manner to represent the total effect of any force or process that slows down the bacteria. It might include, for example, the drag which acts on a body moving in a shallow layer of viscous fluid. It might include the probability that a flagellum will adhere or get tangled with the polymers of the agar. We suggest that the bacterial movement depends on the local lubricant height through a power law with the exponent $\gamma > 0$:

$$\text{movement} = \vec{\nabla} \cdot (D_b (l/l_M)^{\gamma} \vec{\nabla} b), \tag{4}$$

where D_b is a constant with dimensions of a diffusion coefficient and l_M is the maximal height of the lubricant (see below). D_b is related to the fluid's viscosity and the dryness of the agar might affect this viscosity.

Gathering the various terms gives the partial model:

$$\frac{\partial b}{\partial t} = \vec{\nabla} \cdot (D_b (l/l_M)^{\gamma} \vec{\nabla} b) + kbn - \mu b,$$
$$\frac{\partial n}{\partial t} = D_n \nabla^2 n - \alpha k b n, \tag{5}$$
$$\frac{\partial s}{\partial t} = \mu b,$$

where α is a conversion factor, being the amount of nutrient consumed for reproduction of a new bacterium. The third equation in Eq. (5) describes the stationary bacteria. Since they are immotile their dynamics include only a source term: their conversion from the motile state.

This model (with the equation for the lubricant fluid) is capable of producing branched patterns. The dependence of the bacterial diffusion on the lubricant field provides the appropriate mechanism. However, the sporulation term is also

required in order to produce patterns [56]. The lubricant-dependent diffusion affects the front of the bacterial field to form ''fjords.'' With a sporulation term present, bacteria left behind the propagating front become nonmotile. They are unable to move and close the ''fjords,'' thus allowing real branches to form.

We model the dynamics of the lubricating fluid also by a reaction-diffusion equation. There are two reaction terms: production by the bacteria and absorption into the agar. The dynamics of the field are given by

$$\frac{\partial l}{\partial t} = -\vec{\nabla}\cdot\vec{J}_l + f_l(b,n,l) - \lambda l, \tag{6}$$

where $\vec{J}_l$ is the fluid flux (to be discussed), $f_l(b,n,l)$ is the fluid production term, and λ is the absorption rate of the fluid into the agar.

We assume that the fluid production depends on the bacterial density. As the production of lubricant probably demands substantial metabolic efforts, it should also depend on the nutrient's level. We take the simplest case where the production depends linearly on the concentrations of both the bacteria and the nutrients. The exact relation should depend on the synthetic pathway of the active agents composing the lubricant. If they are, for example, secondary metabolites, then their production does not depend on the current nutrient level, but on the prior accumulation of primary metabolites. However, numerical simulations suggest that the model is not sensitive to the exact dependence of the fluid production on the nutrient concentration or even if that dependence is removed.

It is reasonable that the bacteria produce the lubricant up to a height, denoted as l_M, which is sufficient for their swimming motion. Therefore, the production term should have the lubricant height saturate at $l=l_M$. We estimate l_M to be a few microns, which is larger than the width of bacteria (about 0.5μ). This value is based on Numarsky (polarized light) microscopy of colony branches [as in Fig. 2(b)] showing the lubricant height. We take the production term to be

$$f_l(b,n,l) = \Gamma b n (l_M - l), \tag{7}$$

where Γ is the production rate.

We turn to the flow of the lubricating fluid. The physical problem is that of a flow of a complex fluid whose composition is uncertain over a gel-like substance (the agar), while there are immersed in the fluid self-propelling particles of considerable size (the bacteria). A full treatment of the problem would be very complicated. Thus we resort to a simple model of the lubricant flow. Similar (yet simpler) phenomena of the flow of thin films are usually described by a time evolution equation for the height of the fluid (see [65] and references within). Accordingly the flow of the lubricant fluid is described by an equation for its height. As a simple description we assume (without attempting to derive) that the fluid flux can be described as a nonlinear diffusion process:

$$\vec{J}_l = -D_l (l/l_M)^{\nu} \vec{\nabla} l, \tag{8}$$

where D_l is a constant with dimensions of a diffusion coefficient. The diffusion coefficient depends on the height of the fluid to the power $\nu > 0$. The nonlinearity causes the fluid to have a sharp boundary at the front of the colony, as is observed in bacterial colonies. The lubricating fluid flows also by convection caused by bacterial motion. A simple description of the convection is that as each bacterium moves, it drags along with it the fluid surrounding it. However, in simulations that we performed, this feature produced minor effects. We do not include it in the model presented here. Gathering the various terms we obtain the equation for the lubricant field:

$$\frac{\partial l}{\partial t} = \vec{\nabla}\cdot(D_l (l/l_M)^{\nu} \vec{\nabla} l) + \Gamma b n (l_M - l) - \lambda l. \tag{9}$$

The functional form of the terms that we proposed are simple and plausible, but they were not derived from basic physical principles. Therefore, we cannot derive exact relations between the parameters of those terms and the physical properties of the agar substrate. However, we can propose some relations between the parameters and the agar. In the experiments, the agar concentration is controlled. Higher agar concentration gives a dryer and more solid substrate. We shall try to determine the effects on the lubricant layer. We recall that the lubricant fluid is composed of water and of active components such as surfactants. A dryer agar can increase the absorption rate λ. Alternatively, it can diminish the amount of water extracted by the active components. Then either the lubricant layer will be thinner or the bacteria will have to produce more of the active components. The former case should decrease D_b while the latter should decrease the production rate Γ. In both cases the composition of the lubricant fluid will change as the concentration of the active components will increase. The lubricant fluid should become more viscous, with the effect of D_b and D_l decreasing.

Equation (9) together with Eq. (5) form our model. Before further studies of the model we reduce the number of parameters by using dimensionless units. We define the new variables:

$$\begin{gathered} t' = t\mu, \quad \vec{x}' = \vec{x}\sqrt{\mu/D_n}, \quad b' = bk\alpha/\mu, \\ n' = nk/\mu, \quad l' = l/l_M . \end{gathered} \tag{10}$$

With the same units we define

$$\begin{gathered} D_b' = D_b/D_n, \quad D_l' = D_l/D_n, \\ \Gamma' = \Gamma\mu/k^2\alpha, \quad \lambda' = \lambda/\mu, \end{gathered} \tag{11}$$

Using these variables in Eqs. (5) and (9) and omitting the primes we get

$$\begin{aligned} \frac{\partial b}{\partial t} &= \vec{\nabla}\cdot(D_b l^{\gamma} \vec{\nabla} b) + bn - b, \\ \frac{\partial n}{\partial t} &= \nabla^2 n - bn, \\ \frac{\partial l}{\partial t} &= \vec{\nabla}\cdot(D_l l^{\nu} \vec{\nabla} l) + \Gamma b n (1-l) - \lambda l, \\ \frac{\partial s}{\partial t} &= b. \end{aligned} \tag{12}$$

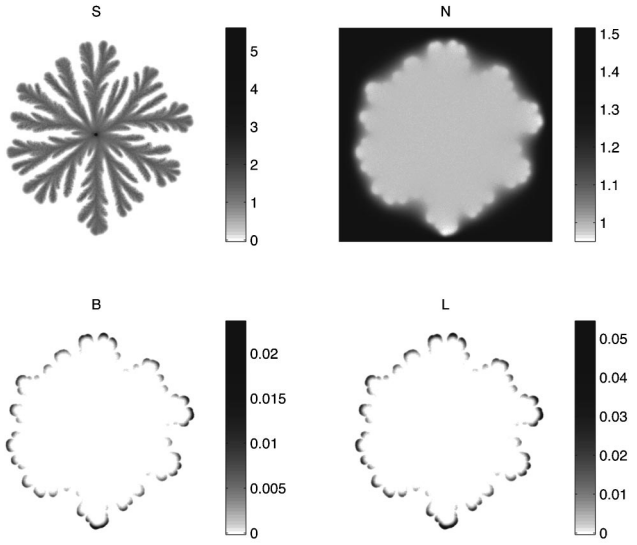

FIG. 4. A representative branching pattern produced by the lubricating bacteria model. The image shows the four fields of the model.

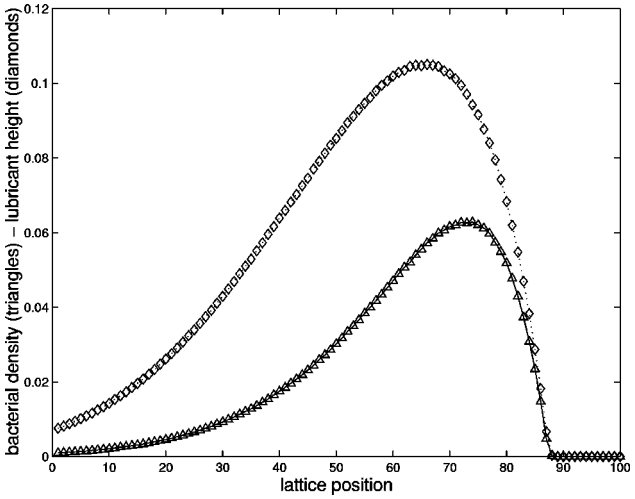

FIG. 5. Profile of the fronts of the bacterial field (triangles) and of the lubricating field (diamonds) from the 2D model. The fields propagate to the right. Both fronts have compact support. The tail of the lubricating field left behind decays more slowly, depending on the parameter λ.

IV. RESULTS OF NUMERIC SIMULATIONS

Figures 4–10 show results of numerical simulations of the model. The figures display the sum of the active and stationary bacterial densities, $b+s$. The simulations were done with an explicit method. To reduce the implicit lattice anisotropy, a quenched noise was introduced into the gradient operator. A noise field $\chi(\vec{x})$ was defined, which assigns to each lattice cell a random value from the interval $(1-\chi_0,1+\chi_0)$, the amplitude being relatively small, $\chi_0=0.005$. The diffusive flux of a field $f(\vec{x},t)$ was computed as

$$\vec{J}_f(\vec{x},t)=-D_f\vec{\nabla}[\chi(\vec{x})f(\vec{x},t)]. \tag{13}$$

For each of the three fields b, n, and l we created a different noise field.

We used a triangular lattice with 350×400 lattice cells. For the initial conditions, we set n to have a uniform distribution of level n_0, b to be zero everywhere but in the center, and the other fields to be zero everywhere.

In Fig. 4 we show the fields s, n, b, and l from a representative simulation. The general features we discuss next are relevant to all the patterns presented in this work. The nutrient field n was consumed by bacteria down to a level of $n\sim1(\mu/k$ in the original units) in the area covered by the colony (the nutrient was not completely depleted due to the functional form of the bacterial sporulation term, the same as in [54] and unlike [53,52]). As the nutrient diffuses faster than the other fields, it also decreased in the area between the colony branches. The field of the motile bacteria b and the lubricant field l are overlapping. The motile bacteria are confined to the area covered by a lubricant. The fronts of both fields have compact support as Fig. 5 shows. Note that as the bacterial and lubricant fields are overlapping (as Figs. 4 and 5 suggest), it is possible to simplify the model. Ben Jacob and Cohen proposed that the coupling of the bacterial motion to the lubricant layer can be replaced by a density-dependent diffusion coefficient for the bacteria $D_b=D_b(b)$ [66,17,56]. If we assume that the local amount of lubricant is a function of the local bacterial density, then we can eliminate the lubricant from the bacterial dynamics and obtain a density-dependent diffusion coefficient. A model of this kind was proposed and studied by Kitsunezaki [54] (that model was derived without referring explicitly to the lubricant layer).

In experiments of bacterial colonies there are two control parameters: the agar concentration and the initial nutrient concentration. First we examined the effect of changing the latter. As Fig. 6 shows, we obtained a dense circular colony when n_0 was large, a branched pattern when we decreased n_0, and a DLA-like pattern when n_0 was close to 1. Similar effects of decreasing the initial nutrient level appear in other reaction-diffusion models [52–54,56].

Changing the agar concentration affects the dynamics of the lubricant fluid. We suggested in the preceding section that a higher agar concentration relates to a larger absorption rate λ and to lower production rate Γ and diffusion coefficients D_l and D_b. It is not *a priori* clear what is the exact dependence of each parameter on the agar concentration. We use the model to investigate this question. In Fig. 7 we show patterns obtained with different values of the parameters Γ and λ. As we expected, increasing λ or decreasing Γ produced a more ramified pattern with thinner branches, similar to the effect of higher agar concentrations on the patterns of bacterial colonies [Fig. 1(a)]. The value of the diffusion coefficient of the lubricating fluid D_l has less influence on the colony pattern, as can be seen in Fig. 8. In contrast, decreasing the bacterial diffusion coefficient D_b produces a ramified pattern, as Fig. 9 shows.

In most of the figures we took $\gamma=1$ and $\nu=1$. There is no *a priori* reason to take these values, and in Fig. 10 we show the effect of other values on the growth. While the patterns are different, we found that these changes can be compensated by other parameters and varying γ and ν has no qualitative effect on the conclusions.

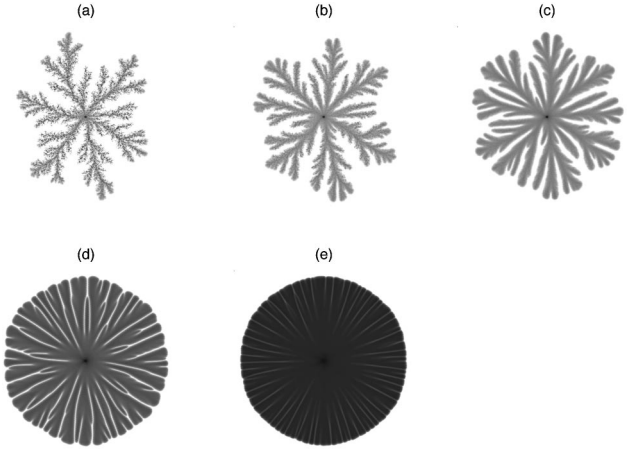

FIG. 6. Effect of varying the initial nutrient concentration n_0 on colony pattern. The minimal value of n_0 to support growth is 1. We include the time t it took for the colony to grow: (a) $n_0=1.1, t=38\,089$, DLA-like pattern; (b) $n_0=1.3, t=11\,410$; (c) $n_0=1.7, t=3671$, branched pattern; (d) $n_0=3, t=721$, dense branches; (e) $n_0=5, t=216$, a disk. The other parameters are $D_b=D_l=0.5, \Gamma=0.6, \lambda=0.1, \gamma=1, \nu=2$.

V. CHEMOTAXIS

The model so far reproduced most of the features of the experimental results displayed in Fig. 1(a), but does not reproduce the transition to ordered patterns at the lowest nutrient concentration (fine radial branches). We will now extend the lubricant model to test for its success in describing this phenomenon. Ben-Jacob *et al.* suggested that this transition is due to chemotaxis and chemotactic signaling [67–69,16]. Chemotaxis means changes in the movement of the bacterium in response to a gradient of certain chemical field [70–73]. The movement is biased along the gradient either in the gradient direction or in the opposite direction. Usually chemotactic response means a response to an externally produced field, as in the case of chemotaxis towards food. However, the chemotactic response can also be to a field produced directly or indirectly by the bacterial cells. We will refer to this case as chemotactic signaling.

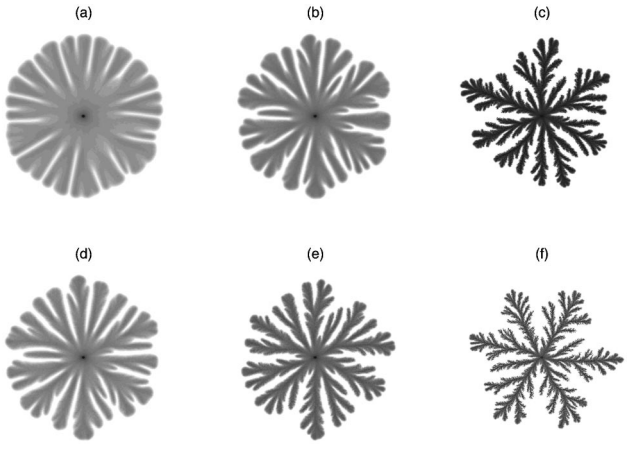

FIG. 7. Effect of varying λ, the fluid absorption rate, on colony pattern. The fluid production rate Γ is 1 in the upper row and 0.3 in the lower row. In both rows λ increases from left to right: $\lambda=0.03$ (left), $\lambda=0.1$ (center), $\lambda=1$ (right). The patterns become more ramified with thinner branches as λ increases. Here and in Figs. 8 and 9 decreasing Γ also produces a more ramified pattern. The other parameters are $D_b=D_l=1, \gamma=\nu=1, n_0=1.5$.

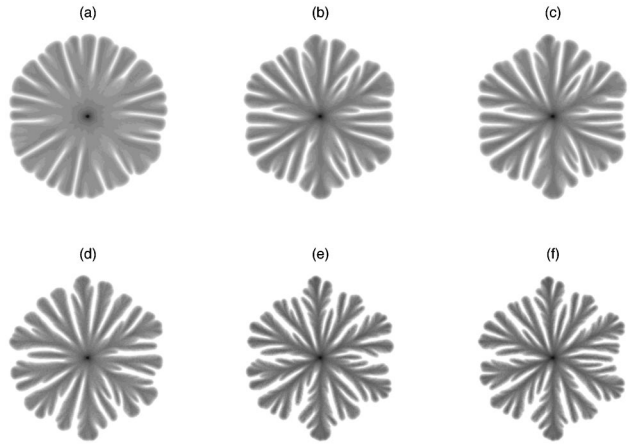

FIG. 8. Effect of varying D_l, the fluid diffusion coefficient, on colony pattern. (a) and (d) are the same as Figs. 7(a) and 7(d). In both rows D_l decreases from left to right: $D_l=1$ (left), $D_l=0.1$ (center), $D_l=0.01$ (right). The patterns do not change significantly.

We incorporate the effect of chemotaxis by introducing a bacterial flux $\vec{J}_{\rm chem}$ due to chemotaxis. The general form is

$$\vec{J}_c=\zeta(l)b\chi(r)\vec{\nabla}r, \tag{14}$$

where the field r represents the concentration of the chemotactic chemical. $\chi(r)\nabla r$ is the gradient sensed by the bacterium [with $\chi(r)$ having units of 1 over the chemical's concentration]. $\chi(r)$ is taken to be the ''receptor law,'' i.e., $\chi(r)=K_r/(K_r+r)^2$ [74]. K_r is a constant that determines the concentration range of the chemical for which the chemotaxis is most effective (K_r is the dissociation constant of the receptor-chemical complex). $\zeta(l)$ (having the same units as a diffusion coefficient) is the bacterial response to the sensed gradient (i.e., the effect on the bacterial movement). In our model the bacterial diffusion coefficient is

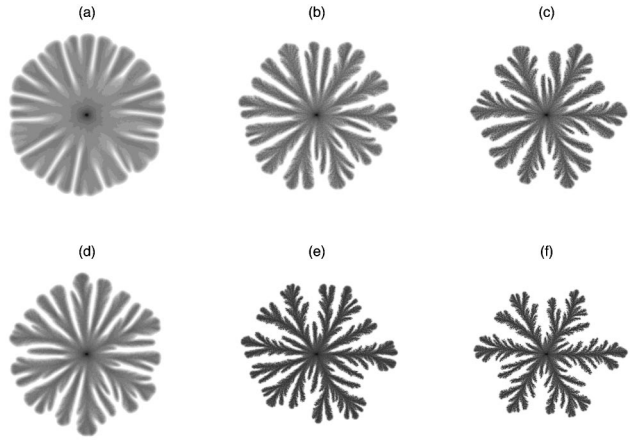

FIG. 9. Effect of varying D_b, the bacterial diffusion coefficient, on colony pattern. (a) and (d) are the same as Figs. 7(a) and 7(d). In both rows D_b decreases from left to right: $D_l=1$ (left), $D_l=0.1$ (center), $D_l=0.05$ (right). The patterns become more ramified as D_b decreases.

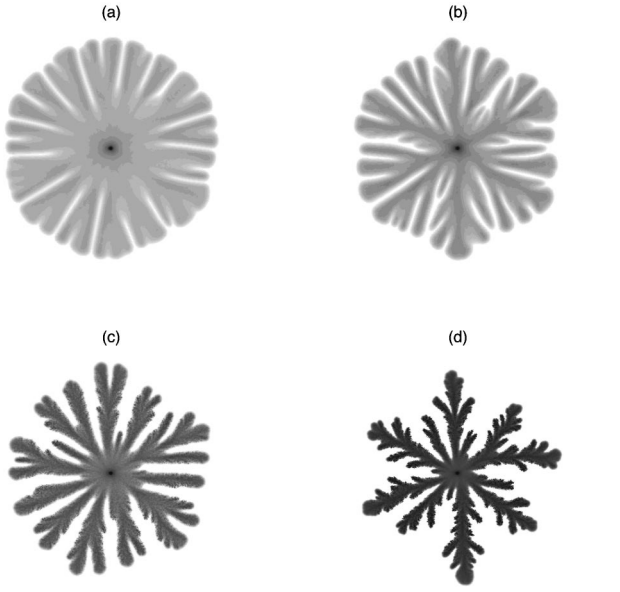

FIG. 10. Effect of changing the exponents γ and ν. We also print the growth time of the colony t. The parameters of the figures are (a) $\gamma=1,\nu=1,t=1249$; (b) $\gamma=1,\nu=2,t=2069$; (c) $\gamma=2,\nu=1,t=4451$; (d) $\gamma=2,\nu=2,t=10\,066$. The other parameters are $D_b=D_l=1,n_0=1.5,\Gamma=1,\lambda=0.03$.

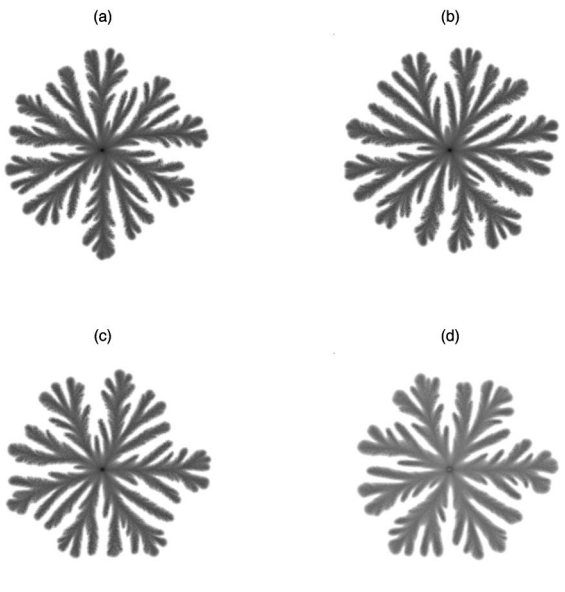

FIG. 11. The effect of food chemotaxis on growth. The four patterns differ in the values of ζ_n, the response to the sensed gradient of the nutrient. We also print the growth time of the colony t: (a) $\zeta_n=0,t=5101$ (no chemotaxis); (b) $\zeta_n=10,t=4957$; (c) $\zeta_n=30,t=3843$; (d) $\zeta_n=100,t=2053$. The other parameters are $D_b=D_l=1,\gamma=\nu=1,n_0=1.5,\Gamma=0.3,\lambda=0.1$.

$D_b l^\gamma$, and the bacterial response to chemotaxis is $\zeta(l)=\zeta_0 D_b l^\gamma$. ζ_0 is a constant, positive for attractive chemotaxis and negative for repulsive chemotaxis.

Amplification of diffusive instability due to nutrient chemotaxis: In nonliving systems, more ramified patterns (lower fractal dimension) are observed for lower growth velocity. Based on growth velocity as a function of nutrient level and based on growth dynamics, Ben-Jacob *et al.* [8] concluded that in the case of bacterial colonies there is a need for a mechanism that can both increase the growth velocity and maintain, or even decrease, the fractal dimension. They suggested food chemotaxis to be the required mechanism. It provides an outward drift to the cellular movements; thus, it should increase the rate of colony propagation. At the same time, being a response to an external field it should also amplify the basic diffusion instability of the nutrient field. Hence, it can support faster growth velocity together with a ramified pattern of low fractal dimension. The bacterial flux due to nutrient chemotaxis is

$$\vec{J}_n \equiv \zeta_n D_b l^\gamma b \frac{K_n}{(K_n+n)^2}\vec{\nabla} n. \tag{15}$$

In Fig. 11 it is shown that, as expected, the inclusion of food chemotaxis led to a considerable increase of the growth velocity without significant change in the fractal dimension of the pattern.

Repulsive chemotactic signaling. We focus now on the formation of the fine radial branching patterns at low nutrient levels. From the study of nonliving systems, it is known that in the same manner that an external diffusion field leads to the diffusion instability, an internal diffusion field will stabilize the growth. It is natural to assume that some sort of chemotactic agent produces such a field. To regulate the organization of the branches, it must be a long-range signal. To result in radial branches it must be a repulsive chemical produced by bacteria at the inner parts of the colony. The most probable candidates are the bacteria entering the prespore state.

As stated above, bacteria may enter a prespore state upon starvation. In this process they emit a wide range of waste materials, some of which are unique to the sporulating bacteria. These emitted chemicals might be used by other bacteria as a signal carrying information about the conditions at the location of the prespores. Ben-Jacob *et al.* [8,75,68] suggested that such materials are repelling the bacteria (''repulsive chemotactic signaling'') as if they escape a dangerous location.

The equation describing the dynamics of the chemorepellent contains terms for diffusion, production by prespores, decomposition by active bacteria, and spontaneous decomposition:

$$\frac{\partial r}{\partial t}=D_r\nabla^2 r+\Gamma_r s-\Omega_r b r-\lambda_r r, \tag{16}$$

where D_r is the diffusion coefficient of the chemorepellent, Γ_r is the emission rate of repellent by prespores, Ω_r is the decomposition rate of the repellent by active bacteria, and λ_r is the rate of self-decomposition of the repellent. The bacterial flux due to repulsive chemotaxis is:

$$\vec{J}_r=\zeta_r D_b l^\nu b\frac{K_r}{(K_r+r)^2}\vec{\nabla} r, \tag{17}$$

where $\zeta_r<0$ (repulsive chemotaxis).

In Fig. 12 the effect of repulsive chemotactic signaling is shown. In the presence of repulsive chemotaxis the patterns have a smooth circular envelope, while the branches are thinner and radially oriented.

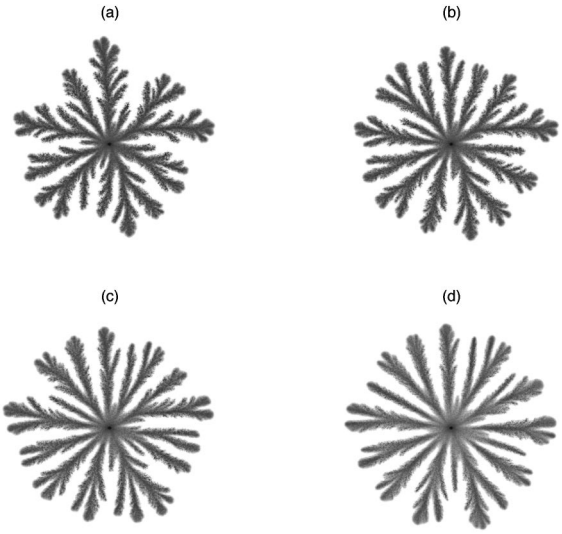

FIG. 12. The effect of repulsive chemotaxis on growth. The four patterns differ in the values of ζ_r, the response to the sensed gradient of the chemorepellent: (a) $\zeta_r=0$ (no chemotaxis), (b) $\zeta_r=-20$, (c) $\zeta_r=-50$, (d) $\zeta_r=-100$. The other parameters are $D_b=D_l=1,\gamma=\nu=1,n_0=1.3,\Gamma=0.3,\lambda=0.1$.

VI. ANOTHER LOOK ON MODELING BACTERIAL GROWTH

The model presented in Sec. III goes along the lines of existing models [54,52] in interpreting the bacterial growth terms (reproduction and sporulation). There are, however, some biological considerations that may have been overlooked. In Sec. III we termed knb as ''reproduction'' and μb as ''sporulation.'' But looking at them term by term reveals discrepancies. The so-called ''sporulation'' term in the equations represents, according to the usual interpretation, a constant probability per time unit for a bacterium to enter the prespore state. This is incompatible with our biological knowledge. A nutritional stress is one of the prerequirements for starting the process of sporulation. As long as there is enough food for the bacteria to reproduce, there is no nutritional stress. In the model it means that as long as the (local) bacterial density increases (i.e., as long as the sum of all the reaction terms is positive), there can be no sporulation.

This leads to a new interpretation of the reaction terms; the resources that the bacteria consume from the nutrient (energy and materials) are utilized for two main processes: to sustain life and to reproduce. Therefore, the reproduction rate should be proportional to the nutrient consumed minus the amount required for life-sustaining activities. We assume that the latter is required by each bacterium at a constant rate, independent of the nutrient level or the bacterial density. We denote that rate by μ, which previously denoted the sporulation rate. Then we have instead of Eq. (2), with $g(b,n)$ denoting the nutrient consumption rate,

$$\text{reproduction}=g(n,b)-\mu b, \tag{18}$$

$$\text{sporulation}=\begin{cases}0 & \text{if reproduction}>0\\ -\text{reproduction} & \text{if reproduction}<0\end{cases}$$
$$=\max(\mu b-g(n,b),0). \tag{19}$$

So far we did not change the model much. All the terms involved in the dynamics remain the same, but we give them new interpretations. Only the dynamics of the field s changed. Since the dynamics of the other fields are decoupled from the field s, the modified model is effectively identical to the previous model.

As we changed the meaning of the bacterial growth terms, we should reconsider their functional form, focusing our attention on the nutrient consumption term $g(n,b)$. The term $g(n,b)=knb$ was taken to be the limit of growth at low nutrient concentration, but it is not *a priori* evident. We suggest that g should have three regimes corresponding to different limits of the nutrient concentration and bacterial density.

(i) There is a maximal growth rate of the bacteria, along with a maximal rate of nutrient consumption, even for optimal conditions. We denote the maximal consumption rate per bacterium as Ω_n.

(ii) When conditions are not optimal and the nutrient concentration is low, it might be the limiting factor. Nutrient consumption is then diffusion-limited and its rate is proportional to $D_n n$ per bacterium, as D_n defines the effective area from which a bacterium consumes food (assuming no other bacteria interfere with this process).

(iii) When the nutrient concentration is low and the bacterial density is high, there is competition between the bacteria, and the amount of nutrient available for each bacterium is proportional to n/b.

As can be seen in Fig. 2(c), the density of bacteria can be quite high and so the third limiting behavior cannot be ignored. The ratio between the nutrient diffusion length and the distance between bacteria $b^{-1/2}$ determines which is the appropriate regime. We take the nutrient consumption rate to be the minimum of the three expressions:

$$g(b,n)=b\,\min(\Omega_n,kn,en/b), \tag{20}$$

where $k=D_n/\alpha$ and e is a constant rate (the min function could have been replaced by a smooth function with the same limits, but we will set it in this way for clarity). We note that the Michaelis-Menten law [74] of $knb/(1+gn)$ has the first two expressions as limits, but does not incorporate the third one. The new model in dimensionless form is

$$\begin{aligned}\frac{\partial b}{\partial t}&=\vec{\nabla}\cdot(D_b l^{\gamma}\vec{\nabla}b)+g(n,b)-b,\\ \frac{\partial n}{\partial t}&=\nabla^2 n-g(n,b),\\ \frac{\partial l}{\partial t}&=\vec{\nabla}\cdot(D_l l^{\nu}\vec{\nabla}l)+\Gamma bn(1-l)-\lambda l,\\ \frac{\partial s}{\partial t}&=\max(b-g(n,b),0),\end{aligned} \tag{21}$$

where $g(n,b)=b\,\min(\Omega_n/\mu,n,(e\alpha/\mu)(n/b))$. The same transformation of variables (10) and (11) was employed to obtain the dimensionless model.

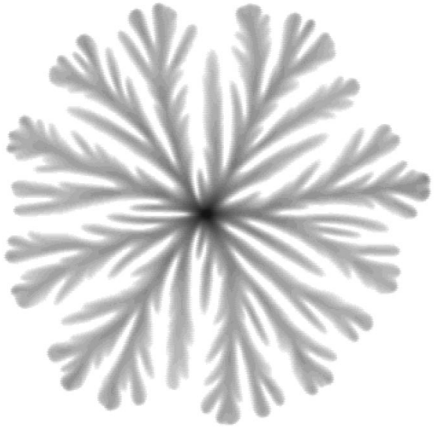

FIG. 13. A pattern produced by the modified model of Sec. VI.

Numerical simulations of the above model show (Fig. 13) no qualitative differences from the model presented in Sec. IV. It is not the mathematical model which is important in this respect, but our understanding of the biological system. This emphasizes the differences between the ''generic modeling'' approach and the approach driving the ''reminiscence syndrome.''

VII. CONCLUSION

We first briefly reviewed experimental observations of branching patterns in bacteria of the species *Paenibacillus*. Both colonial patterns and optical microscope observations of the bacterial dynamics were presented.

Our goal in this paper was to test a new reaction-diffusion model which includes a time-evolution equation of a lubricant. From a comparison of the model simulation and experimental observations we conclude that when a specific bacterial strain is considered, such comparison is not sufficient to tell us if indeed the right biological features are included in the model.

For a more critical test of the models, additional aspects of the growth (such as functional dependence of the colonial growth velocity on growth conditions, branches size and width distributions, etc.) have to be compared with the model's predictions. One should also compare the theory with more involved experimental tests, such as the effect of imposed anisotropy, competition between neighboring colonies, and expression of mutants (emergence of sectors) in expanding colonies.

Our conclusion from the study of bacterial branching growth is that the minimal features of diffusion, food consumption, reproduction, and inactivation are not sufficient to explain the complete picture of the observed phenomena. We believe that additional mechanisms must be introduced, and we propose chemotactic signaling as a plausible one.

This work has dealt with a continuous model. Such models are not preferable to discrete ones. Each has its advantages and disadvantages. The discrete walkers model, for example, enables us to include the valuable feature of internal degrees of freedom, but is computationally limited in the number of walkers that can be simulated, and thus its scaling to the real problem is somewhat problematic. The best strategy is to employ in parallel both the reaction-diffusion and the walkers approaches.

[1] T. Matsuyama, K. Kaneda, Y. Nakagawa, K. Isa, H. Hara-Hotta, and I. Yano, J. Bacteriol. **174**, 1769 (1992).
[2] N.H. Mendelson and B. Salhi, J. Bacteriol. **178**, 1980 (1996).
[3] J.O. Kessler, Contemp. Phys. **26**, 147 (1985).
[4] H. Fujikawa and M. Matsushita, J. Phys. Soc. Jpn. **58**, 3875 (1989).
[5] T.J. Pedley and J.O. Kessler, Sci. Prog. **76**, 105 (1989).
[6] E. Ben-Jacob, H. Shmueli, O. Shochet, and A. Tenenbaum, Physica A **187**, 378 (1992).
[7] T. Matsuyama, R.M. Harshey, and M. Matsushita, Fractals **1**, 302 (1993).
[8] E. Ben-Jacob, O. Shochet, A. Tenenbaum, I. Cohen, A. Czirók, and T. Vicsek, Nature (London) **368**, 46 (1994).
[9] E. Ben-Jacob, I. Cohen, O. Shochet, I. Aronson, H. Levine, and L. Tsimering, Nature (London) **373**, 566 (1995).
[10] D.E. Woodward, R. Tyson, M.R. Myerscough, J.D. Murray, E.O. Budrene, and H.C. Berg, Biophys. J. **68**, 2181 (1995).
[11] E. Ben-Jacob, I. Cohen, A. Czirók, T. Vicsek, and D.L. Gutnick, Physica A **238**, 181 (1997).
[12] J. O. Kessler and M. F. Wojciechowski, in *Bacteria as Multicellular Organisms*, edited by J. A. Shapiro and M. Dworkin (Oxford University Press Inc., New York, 1997), pp. 417–450.
[13] S.E. Esipov and J.A. Shapiro, J. Math. Biol. **36**, 249 (1998).
[14] M. Doudoroff, R. Y. Stainer, and E. A. Adelberg, *The Microbial World* (Prentice-Hall, Englewood Cliffs, NJ, 1957).
[15] J.A. Shapiro, Science **258**(6), 62 (1988).
[16] E. Ben-Jacob, Contemp. Phys. **38**, 205 (1997).
[17] E. Ben-Jacob, I. Cohen, and H. Levine, Adv. Phys. (to be published)
[18] H. Levine and E. Ben-Jacob, Sci. Am. **279** (4), 82 (1998).
[19] N.H. Mendelson Proc. Natl. Acad. Sci. USA **75**, 2478 (1978).
[20] P. Devreotes, Science **245**, 1054 (1989).
[21] R.M. Harshey, Mol. Microbiol. **13**, 389 (1994).
[22] W.C. Fuqua, S.C. Winans, and E.P. Greenberg, J. Bacteriol. **176**, 269 (1994).
[23] A Latifi, M.K. Winson, M. Foglino, B.W. Bycroft, G.S. Stewart, A. Lazdunski, and P. Williams, Mol. Microbiol. **17**, 333 (1995).
[24] C. Fuqua, S.C. Winans, and E.P. Greenberg, Annu. Rev. Microbiol., **50**, 727 (1996).
[25] E.O. Budrene and H.C. Berg, Nature (London) **349**, 630 (1991).
[26] Y. Blat and M. Eisenbach, J. Bacteriol. **177**, 1683 (1995).
[27] E.O. Budrene and H.C. Berg, Nature (London) **376**, 49 (1995).
[28] J.A. Shapiro and D. Trubatch, Physica D **49**, 214 (1991).
[29] B. Salhi and N.H. Mendelson, J. Bacteriol. **175**, 5000 (1993).
[30] T. Galitski and J.R. Roth, Science **268**, 421 (1995).
[31] J.P. Rasicella, P.U. Park, and M.S. Fox, Science **268**, 418 (1995).
[32] R. V. Miller, Sci. Am. **278** (1), 66 (1998).

[33] M. Matsushita and H. Fujikawa, Physica A **168**, 498 (1990).
[34] H. Fujikawa and M. Matsushita, J. Phys. Soc. Jpn. **60**, 88 (1991).
[35] R.N. Smith and F.E. Clacrk, J. Bacteriol. **35**, 59 (1938).
[36] T. H. Henrici, *The Biology of Bacteria: The Bacillaceae*, 3rd ed. (D. C. Heath & Company, Boston, MA, 1948).
[37] T.A. Witten and L.M. Sander, Phys. Rev. Lett. **47**, 1400 (1981).
[38] L.M. Sander, Nature (London) **322**, 789 (1986).
[39] T. Vicsek, *Fractal Growth Phenomena* (World Scientific, New York, 1989).
[40] T. Matsuyama and M. Matsushita, *Morphogenesis by Bacterial Cells*, in *Fractal Geometry in Biological Systems, An Analytical Approach*, edited by P. M. Iannacone and M. K. Khokha (CRC Press, New York, 1995), pp. 127–171.
[41] E. Ben-Jacob, A. Tenenbaum, O. Shochet, and O. Avidan, Physica A **202**, 1 (1994).
[42] M. Tcherpakov, E. Ben-Jacob, and D. Gutnick, Int. J. Syst. Bacteriol. **49**, 239 (1999).
[43] E. Ben-Jacob, I. Cohen, and D. Gutnick, Annu. Rev. Microbiol. **52**, 779 (1998).
[44] T. Matsuyama and M. Matsushita, Crit. Rev. Microbiol. **19**, 117 (1993).
[45] J. Horgan, Sci. Am. **272** (6), 104 (1995).
[46] D.A. Kessler and H. Levine, Phys. Rev. E **48**, 4801 (1993).
[47] M.Y. Azbel, Europhys. Lett. **22**, 311 (1993).
[48] E. Ben-Jacob, I. Cohen, O. Shochet, A. Czirók, and T. Vicsek, Phys. Rev. Lett. **75**, 2899 (1995).
[49] D.A. Kessler, H. Levine, and L. Tsimring, Physica D **106**, 375 (1997).
[50] H. Parnas and L. Segel, J. Theor. Biol. **71**, 185 (1978).
[51] S.A. Mackay, J. Cell. Sci. **33**, 1 (1978).
[52] M. Matsushita, J. Wakita, H. Itoh, I. Rafols, T. Matsuyama, H. Sakaguchi, and M. Mimura, Physica A **249**, 517 (1998).
[53] K. Kawasaki, A. Mochizuki, M. Matsushita, T. Umeda, and N. Shigesada, J. Theor. Biol. **188**, 177 (1997).
[54] S. Kitsunezaki, J. Phys. Soc. Jpn. **66**, 1544 (1997).
[55] I. Rafols, M.Sc. thesis, Chuo University, Japan, 1998.
[56] I. Golding, Y. Kozlovsky, I. Cohen, and E. Ben-Jacob, Physica A **260**, 510 (1998).
[57] M.A. Marahiel, M.M. Nakano, and P. Zuber, Mol. Microbiol **7**, 631 (1993).
[58] J.D. Desai and I.M. Banat, Microbiol. Mol. Biol. Rev. **61**, 47 (1997).
[59] T. Matsuyama and Y. Nakagawa, Colloids Surf., B **7**, 207 (1996).
[60] S.J. Stahl, K.R. Stewart, and F.D. Williams, J. Bacteriol. **154**, 930 (1983).
[61] D.A. Kessler, J. Koplik, and H. Levine, Adv. Phys. **37**, 255 (1988).
[62] J.S. Langer, Science **243**, 1150 (1989).
[63] E. Ben-Jacob and P. Garik, Nature (London) **343**, 523 (1990).
[64] E. Ben-Jacob, Contemp. Phys. **34**, 247 (1993).
[65] N. Samid-Merzel, S.G. Lipson, and D.S. Tannhauser, Phys. Rev. E **57**, 2906 (1998).
[66] I. Cohen, Master's thesis, Tel-Aviv University, 1997 (unpublished).
[67] E. Ben-Jacob, I. Cohen, and A. Czirók, *Smart Bacterial Colonies*, in *Physics of Biological Systems: From Molecules to Species*, Lecture Notes in Physics (Springer-Verlag, Berlin, 1997), pp. 307–324.
[68] I. Cohen, A. Czirók, and E. Ben-Jacob, Physica A **233**, 678 (1996).
[69] E. Ben-Jacob and I. Cohen, *Cooperative formation of bacterial patterns*, in *Bacteria as Multicellular Organisms*, edited by J. A. Shapiro and M. Dworkin (Oxford University Press, New York, 1997).
[70] J. Adler, Science **166**, 1588 (1969).
[71] H.C. Berg and E.M. Purcell, Biophys. J. **20**, 193 (1977).
[72] *Biology of the Chemotactic Response*, edited by J. M. Lackiie (Cambridge University Press, Cambridge, 1986).
[73] H. C. Berg, *Random Walks in Biology* (Princeton University Press, Princeton, NJ, 1993).
[74] J. D. Murray, *Mathematical Biology* (Springer-Verlag, Berlin, 1989).
[75] E. Ben-Jacob, O. Shochet, A. Tenenbaum, I. Cohen, A. Czirók, and T. Vicsek, Fractals **2**, 15 (1994).